Self-normalized photothermal techniques for thermal diffusivity measurements

J. A. Balderas-López[a] and A. Mandelis[b]
Photothermal and Optoelectronic Diagnostics Laboratories (PODL), Department of Mechanical and Industrial Engineering, University of Toronto, 5 King's College Road, Toronto, Ontario M5R 3G8, Canada

(Received 22 June 2000; accepted for publication 19 September 2000)

Two self-normalized photothermal techniques, to carry out thermal diffusivity measurements of condensed phase materials, are presented. These simple methodologies involve linear fitting procedures of the signal amplitude and phase. These procedures lead to the elimination of the usual requirement for instrumental transfer-function normalization. The thermal diffusivities for two dental resins and two pure liquids are measured with these simple methodologies and very good agreement is found with values reported in the literature, where more involved analysis is usually required. © *2000 American Institute of Physics.* [S0021-8979(00)08124-X]

I. INTRODUCTION

Photothermal techniques have found extensive applications in various areas of science and engineering. Nowadays they are used in a wide range of scientific disciplines to carry out studies of diverse properties of condensed matter.[1–6] Among the main applications of these techniques, the thermal characterization of substances, both in liquid and solid phases,[4–10] is widely used. In particular, photoacoustic and photopyroelectric techniques have become very popular owing to their simplicity, including minimal or no sample preparation requirements.[4–12]

A major problem to overcome when using photothermal techniques in the frequency domain is how to deal with the instrumental transfer function, which is quite difficult or even impossible to model theoretically. A recently reported photoacoustic analytical procedure involves modeling of this transfer function,[9,10] then using the model for fitting to experimental data. This method, however, has high inherent uncertainty. Other methodologies involve various data normalization procedures.[4,8]

In this work two alternate photothermal self-normalization methodologies are presented. One procedure relies solely on experimental data normalization by taking the ratio of signal amplitudes from two samples of the same material and different thicknesses. With this self-normalization procedure the instrumental transfer function is automatically eliminated. This methodology was implemented using gas-microphone photoacoustics in the open photoacoustic configuration (OPC) to the measurement of the thermal diffusivity of two dental resins. Another procedure which does not require samples of different thicknesses relies on obtaining self-normalized frequency scans in liquids by means of photopyroelectric detection using a thermal wave resonator cavity (TWRC) and frequency scans for two different cavity lengths. The instrumental transfer function is automatically eliminated by forming ratios of amplitudes and differences of phases for each cavity length. This method is demonstrated with two pure liquids (distilled water and ethylene glycol).

II. THEORY

A. Photoacoustic self-normalization

In consideration of the optically opaque (surface-absorption) limit[13] it can be shown that the complete photoacoustic signal in the OPC configuration is given by the expression[11]

$$\delta P(f,L)=\frac{Y}{\sigma_g\sigma_s}\frac{1}{\sinh(L\sigma_s)}\left[1+\frac{2A}{\sigma_s}\left\{\cosh(L\sigma_s)-\frac{L\sigma_s}{2}\sinh(L\sigma_s)-1\right\}\right]. \tag{1}$$

In this equation Y is a coefficient involving geometrical parameters, as well as optical and thermal properties. The parameter A involves the linear expansion coefficient α_T, its magnitude being determined by the thermoelastic behavior of the sample. L is the sample thickness, and $\sigma_j=(1+i)\sqrt{\pi f/\alpha_j}$, $j=g$, s, is the complex thermal diffusion coefficient, where f is the optical-source modulation frequency and α_j is the thermal diffusivity of the jth substance. The letter g refers to the *g*as inside the photoacoustic chamber; s refers to the optically absorbing sample.

Equation (1) is often too complicated to be used for analytical purposes. Some approximations based on the value of the dimensionless parameter $x=(f/f_c)^{1/2}$, where $f_c=\alpha_s/\pi L^2$ is the critical frequency, are more useful. This is the frequency at which the thermal diffusion length $\mu_s=|\sigma_s|/\sqrt{2}$ is equal to the thickness of the sample. Depending on the value of the dimensionless parameter x, the photothermal behavior of the sample lies between the entirely thermally thin ($x\ll 1$) and entirely thermally thick regime ($x\gg 1$). In this work, we consider the quasithermally thick regime, defined for the condition $x>1$.[13] This allows the monitoring of measurable thermal-wave power in transmission.

[a]On leave from Centro de Investigación en Ciencia Aplicada y Tecnología Avanzada del IPN, Av. Legaria 694, Col. Irrigación, C.P. 11500, México, D. F., México.
[b]Electronic mail: mandelis@mie.utoronto.ca

 © 2000 American Institute of Physics

Downloaded 18 Jul 2008 to 128.100.49.17. Redistribution subject to AIP license or copyright; see http://jap.aip.org/jap/copyright.jsp

Furthermore, depending on the linear thermal expansion coefficient and thickness of the sample [included in the parameter A in Eq. (1)], a thermoelastic contribution may appear in the quasithermally thick and thermally thick regimes.[12] If this contribution can be separated out at higher frequencies, as is the case with our photoacoustic experiments, it may be theoretically ignored. Then the OPC amplitude, Eq. (1), is simplified substantially in the quasithermally thick regime.[9–11] The resulting expression is

$$\delta P(f,L)=c(f)\frac{e^{-a\sqrt{f}}}{f}. \tag{2}$$

Here, the coefficient $c(f)$ contains the instrumental transfer function and is independent of the samples thickness. The parameter a is defined as $a=L(\pi/\alpha_s)^{1/2}$. By taking the ratio of Eq. (2) with itself for two different sample thicknesses L_1 and L_2, it is clear that the term $c(f)$ is eliminated, yielding the simpler expression

$$R(f)=\frac{\delta P^2}{\delta P^1}=e^{-B\sqrt{f}}. \tag{3}$$

Therefore, the thermal diffusivity of the sample can be obtained from knowledge of the parameter B, defined as $B=(L_2-L_1)(\pi/\alpha_s)^{1/2}$. The measurement procedure involves ratioing the photoacoustic amplitudes obtained in transmission experiments from two samples of different thicknesses and plotting them versus the square root of the modulation frequency, followed by the corresponding linear best fit on a semi-log scale to obtain the slope of the straight line.

B. Photopyroelectric self-normalization

According to the mathematical theory of the TWRC,[7,14] it has been shown that the pyroelectric signal from this device, Fig. 1 is given by

$$V(f,L)=C(f)\times\frac{e^{-\sigma_l L}}{1-\gamma_{ls}\gamma_{lp}e^{-2\sigma_l L}}, \tag{4}$$

where V is the pyroelectric voltage output in the open-circuit configuration, L is the cavity length, and σ_l is the complex thermal diffusion coefficient, as defined before. In this definition α_l is the thermal diffusivity of the intracavity medium (a liquid sample in our case). The interfacial thermal coefficients γ_{jk} are defined as

$$\gamma_{jk}=\frac{(1-b_{jk})}{(1+b_{jk})}, \tag{5}$$

where $b_{jk}=e_j/e_k$ is a thermal coupling coefficient, the ratio of thermal effusivities of media j and k; the subscripts s, p, and l refer to the thermal-wave source (a plane metallic light absorber, such as a copper or aluminum strip; see Fig. 1), the pyroelectric material and the liquid sample, respectively. The term $C(f)$, involving the transfer function, is a complex expression containing parameters such as the laser intensity, the thin-layer thermal wave source thickness (in this case aluminum foil), and the thermal properties of the substances involved (the liquid sample and the air surrounding the cavity). $C(f)$ is independent of the cavity length (sample thickness). Then, by taking the ratio of Eq. (4) for two different cavity lengths is clear that the $C(f)$ term is eliminated. Moreover, the higher-order thermal-wave superpositions in the denominator may be neglected in our experiment, the product of the interfacial thermal coupling coefficients γ_{jk}

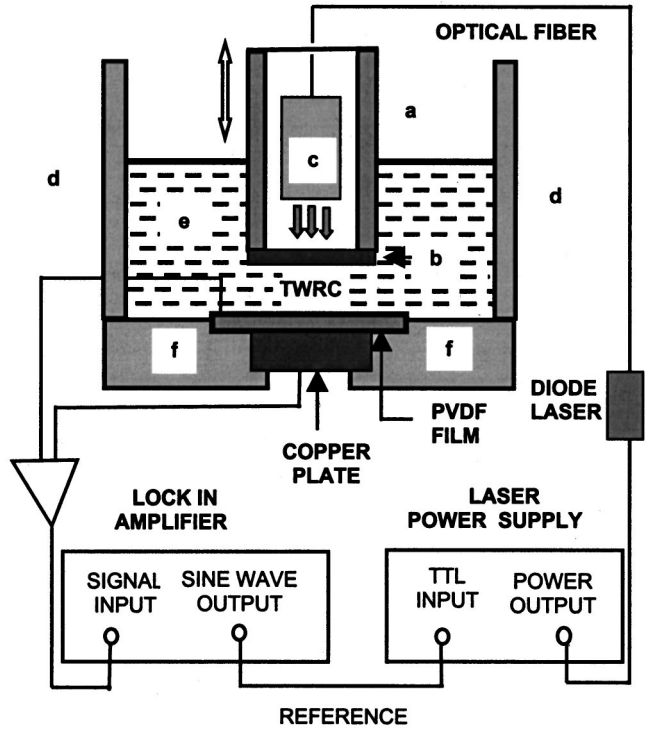

FIG. 1. Schematic cross section of the TWRC configuration experimental setup used for self-normalized thermal diffusivity measurements of liquids. (a) Cylindrical thermal-wave emitter head containing the aluminum foil absorber (b), and the photothermal chamber with the optical fiber (c). (d) Container walls. (e) Liquid sample filling the thermal wave resonator cavity (TWRC). (f) Dielectric substrate. The bottom surface of the PVDF was attached to a copper plate, this plate worked as electric contact and support.

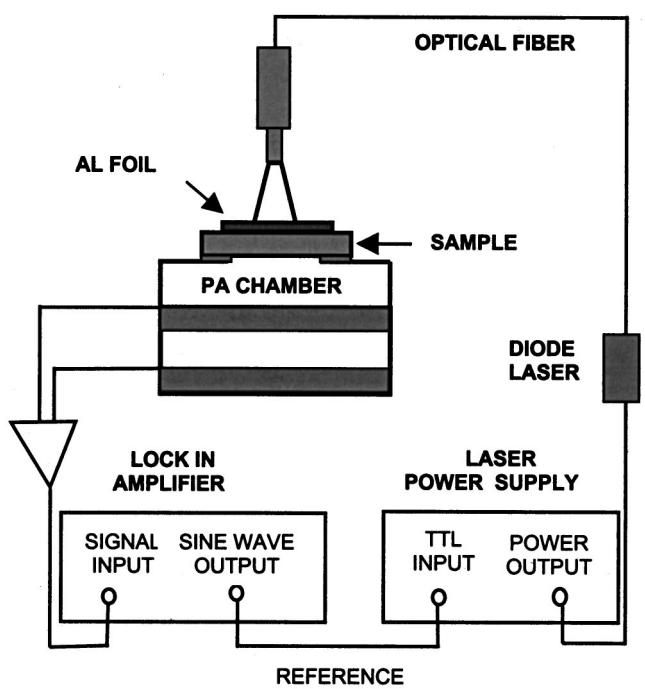

FIG. 2. Schematic cross section of the OPC configuration experimental setup used for self-normalized thermal diffusivity measurements of solids.

Downloaded 18 Jul 2008 to 128.100.49.17. Redistribution subject to AIP license or copyright; see http://jap.aip.org/jap/copyright.jsp

TABLE I. Thermal diffusivities for two pure liquids, measured using the TWRC methodology, and corresponding values reported in the literature.

Liquid sample	Thickness cm ($\times 10^{-2}$)	$\Delta L_{ji}=L_j-L_I$ cm ($\times 10^{-2}$)	α_{Amp} cm^2/s ($\times 10^{-2}$)	α_{Phase} cm^2/s ($\times 10^{-2}$)	α_{Ref} cm^2/s ($\times 10^{-2}$)
distilled	$L_1=2.00\pm0.005$	$\Delta L_{21}=0.5\pm0.007$	0.149 ± 0.006	0.145 ± 0.004	
water	$L_2=2.50\pm0.005$	$\Delta L_{31}=1.0\pm0.007$	0.147 ± 0.004	0.144 ± 0.005	0.1465 (Ref. 18)
($T=26$ °C)	$L_3=3.00\pm0.005$	$\Delta L_{32}=0.5\pm0.007$	0.147 ± 0.005	0.143 ± 0.003	(25.7 °C)
ethylene	$L_1=2.00\pm0.005$	$\Delta L_{21}=0.5\pm0.007$	0.098 ± 0.004	0.099 ± 0.003	
glycol	$L_2=2.50\pm0.005$	$\Delta L_{31}=1.0\pm0.007$	0.096 ± 0.005	0.096 ± 0.004	0.0939 (Ref. 19)
($T=30$ °C)	$L_3=3.00\pm0.005$	$\Delta L_{32}=0.5\pm0.007$	0.093 ± 0.003	0.092 ± 0.004	(20 °C)

and the exponential term in the denominator of Eq. (4) is $\ll 1$: For instance, by taking water for reference, with thermal diffusivity 0.001 45 cm^2/s, the magnitude of this term is 0.000 15 for a 0.03 cm cavity length and 5 Hz. The following simple expressions for the magnitude and phase are thus obtained:

$$|V(f)|\approx e^{-A_l\Delta L}, \tag{6}$$

$$\Phi(f)=-A_l\Delta L. \tag{7}$$

Here, $A_l=(\pi f/\alpha_l)^{1/2}$ and $\Delta L=L_2-L_1$. Clearly for a given intracavity medium and judiciously chosen cavity lengths, it is always possible to find a frequency modulation range in which this (quasithermally thick) approximation is valid. Equations (6) and (7) show that it is possible to carry out simple TWRC measurements of the thermal diffusivity of liquids by monitoring the polyvinylidene fluoride (PVDF) signal output as a function of the modulation frequency. The procedure involves, for the amplitude, the PVDF signal at two different cavity lengths and the fitting of the data ratio to a linear equation in a semi-log scale as a function of the square root of the modulation frequency. The same procedure is applicable to the difference of the photothermal phases at the same two different cavity lengths. The thermal diffusivity of the substance is obtained, in both cases, from the slope fitting parameter $P=\Delta L(\pi/\alpha_l)^{1/2}$. Furthermore, the photopyroelectric signal is independent of the thermoelastic properties of the medium when the PVDF sensor operates in the purely pyroelectric mode.

III. EXPERIMENT

The experimental setups are shown in Figs. 1 and 2. They consisted of an infrared laser diode source with a fiber-optic pigtail (Omnicrome Corporation, model OPC-A001-FC/100, 830 nm), operating at 200 mW. The photoacoustic transmission configuration (Fig. 2) was realized by using the sample to cap (and hermetically seal) the chamber of a commercial electret microphone with a built-in preamplifier. The corresponding TWRC configuration (Fig. 1) was obtained by using an aluminum foil (80 μm thickness) as thermal wave generator. The thermal wave generated photothermally on this aluminum foil was launched across the sample thickness and reached the PVDF sensor, located parallel to, and across from, the aluminum foil. The aluminum foil was mounted on a microstage to allow changing its relative distance from the PVDF surface[7] (cavity length).

The lock-in amplifier (LIA) demodulated photothermal signal for both configurations was obtained as a function of the laser-beam-intensity modulation frequency. The laser intensity was modulated using the internal oscillator of the LIA to drive the laser power supply via a TTL communication port. This same signal further comprised the internal reference wave form for the LIA. The liquid temperature for the TWRC setup was measured by means of a thermocouple attached very near the resonator cavity. The maximum temperature increment registered inside the liquid during our experiments was one degree. The temperatures registered in Table I correspond to the one measured by this means. The corresponding sample temperature for the photoacoustic setup was not measured due to practical difficulties in attaching the thermocouple to the sample without disturbing the laser light fluence. Nevertheless the temperature increment was estimated to be 2° or 3°.

IV. RESULTS AND DISCUSSION

The photoacoustic and photopyroelectric methodologies were applied to the measurement of the thermal diffusivity of two pure liquids (Table I), and two dental resins (Table II), respectively.

A. Photoacoustic analysis

The resin samples were prepared in a disk form (1 cm in diameter) with thicknesses between 80 and 200 μm (Table II). To satisfy the surface absorption condition, a piece of aluminum foil (17 μm thick) was attached with thermal paste to the various specimens. The thermal thickness of the foil was thus negligible compared to the sample thicknesses. Figure 3 shows typical photoacoustic signal amplitudes for the

TABLE II. Thermal diffusivities for two dental resins, measured using the self-normalized OPC photoacoustic configuration, and the corresponding values for three similar dental resins reported in the literature.

Dental resin (commercial name)	Thickness cm ($\times 10^{-2}$)	$\Delta L=L_2-L_1$ cm ($\times 10^{-2}$)	α cm^2/s ($\times 10^{-2}$)
3M Resin	$L_1=1.39\pm0.04$		
	$L_2=1.87\pm0.05$	0.48 ± 0.06	0.45 ± 0.09
Degufill H Resin	$L_1=0.86\pm0.03$		
	$L_2=1.70\pm0.05$	0.84 ± 0.06	0.34 ± 0.06
Bonfill	⋯	⋯	0.12 ± 0.02 (Ref. 16)
Adaptic	⋯	⋯	0.68 ± 0.03 (Ref. 16)
Prisma-Fil Dentsply	⋯	⋯	0.50 ± 0.02 (Ref. 17)

Downloaded 18 Jul 2008 to 128.100.49.17. Redistribution subject to AIP license or copyright; see http://jap.aip.org/jap/copyright.jsp

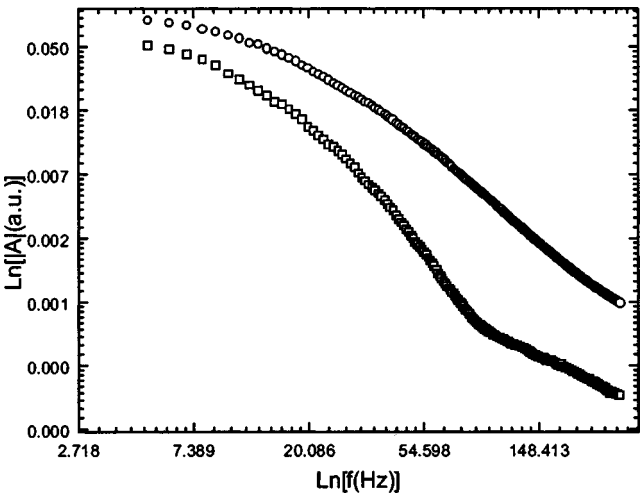

FIG. 3. Typical photoacoustic signal amplitudes for the resins used in this work. Circles correspond to a Degufill H resin (0.0086 cm thickness); squares correspond to another Degufill H sample (0.0170 cm thickness).

two dental resins. Figure 4 shows the ratio of the two photoacoustic amplitudes (thick sample: numerator; thin sample: denominator) on a semi-log scale as a function of the square root of the modulation frequency for one of the resins. The first part of this curve shows the gradual change from the thermally thin regime to the quasithermally thick regime. This change is followed by an inflexion point in the figure. The decreasing, not entirely linear, ratio in the low-frequency portion of this graph is due to the fact that both samples are quasithermally thick and the thermal-wave attenuation rate of the transmission-mode photoacoustic signal amplitude from the thick solid is faster than that of the thin solid. This makes the amplitude ratio decrease. This behavior is followed by the thermoelastic domination of the signal at high modulation frequencies.[12,15] Here the oscillatory thermal expansion of the thin sample is proportionally smaller than that of the thick sample ($\Delta L_j \propto L_j$). As a result, the acoustic vibration amplitude in the photoacoustic chamber is

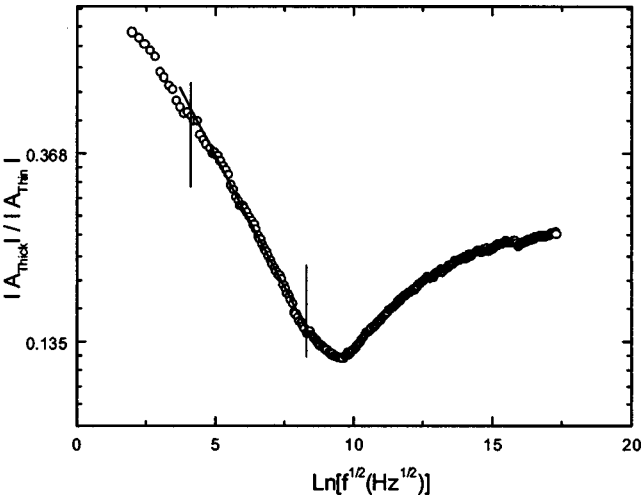

FIG. 4. Photoacoustic signal amplitude ratio for the Degufill H resin samples of Fig. 3. The semilinear behavior in the quasithermally thick regime is delineated by two vertical lines. The continuous straight line is the best fit to Eq. (3) within this region.

stronger for the thick sample and the ratio reverses its direction. The turning point of the curve in Fig. 4 can be used, in principle, to determine the coefficient of thermal expansion of the material constituting the two samples.

The linear behavior on a semi-logarithmic plot in the quasithermally thick region is as predicted from Eq. (3). The superposed straight line in Fig. 4 represents the theoretical best fit to that equation. This fitting was done over the experimental data between the two inflexion points defining the changes on the photoacoustic regimes (from thermally thin to quasithermally thick and quasithermally thick to thermoelastic regimes). The results of the analysis are summarized in Table II. The reported standard deviation was calculated as the experimental error on the B value in Eq. (3) by using the standard formula for error propagation. A comparison of the thermal diffusivity values measured photoacoustically in this work with corresponding values reported in the literature,[16,17] Table II, for similar dental resins reveals reasonable order-of-magnitude agreement. The simplicity of the presented technique is evident when compared with the methodologies used to obtain the values reported in Refs. 16 and 17. One of these methodologies[16] involves measurements of the temperature evolution on a rectangular prism molded specimen, with a thermocouple embedded in it as immersed in a thermal bath. The other methodology[17] is a photoacoustic technique using the phase signal. It involves a procedure to take into account the inherent phase characteristics of the electronic system and careful sample preparation to avoid, as much as possible, acoustic contributions to the photoacoustic signal. It should be mentioned that all methodologies used for the results of Table II exhibit two-digit precision, however, the precision of the present photoacoustic methodology can be improved by suppressing the thermoelastic contribution. To achieve this, limits on the sample maximum thickness must be set. For samples with small linear expansion coefficients the precision is expected to improve.

In principle, the photacoustic phase difference in the thermally thick regime can also be used to derive the thermal diffusivity of the dental resins in Table II. In practice, unfortunately, the photoacoustic phase turns out to be more sensitive to the thermoelastic contribution and this mechanism cannot be easily neglected, as is the case for the amplitude.

B. Photopyroelectric analysis

Figure 5 shows the signal magnitude as a function of the modulation frequency for distilled water, and for three different sample thicknesses, with a 50 μm thickness increment cavity length (Table I). For the analysis, ratios of signal amplitudes for these three different cavity lengths were taken. The corresponding data were plotted as a function of the square root of the modulation frequency. The graph for distilled water is shown in Fig. 6. It is evident from this figure that the linear relationship expected on a semi-logarithmic plot from Eq. (6) is valid throughout the entire frequency range. The continuous lines on the same graph are the best fits to this equation.

Downloaded 18 Jul 2008 to 128.100.49.17. Redistribution subject to AIP license or copyright; see http://jap.aip.org/jap/copyright.jsp

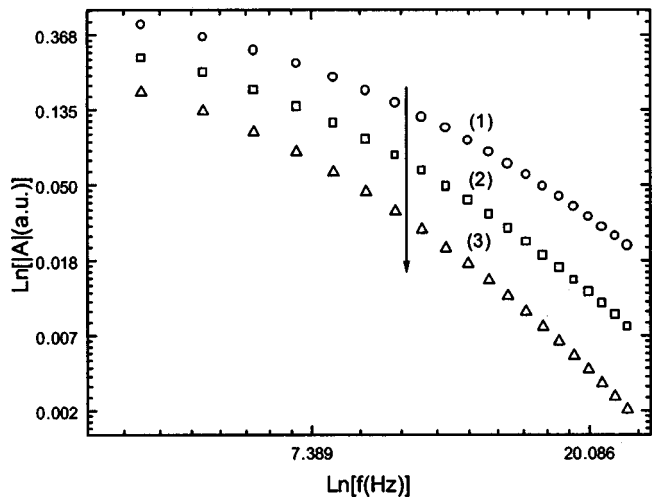

FIG. 5. TWRC signal amplitudes for distilled water at three different intracavity sample thicknesses. Cavity length increases in the direction of the arrow. The differences between these thicknesses are 50 μm.

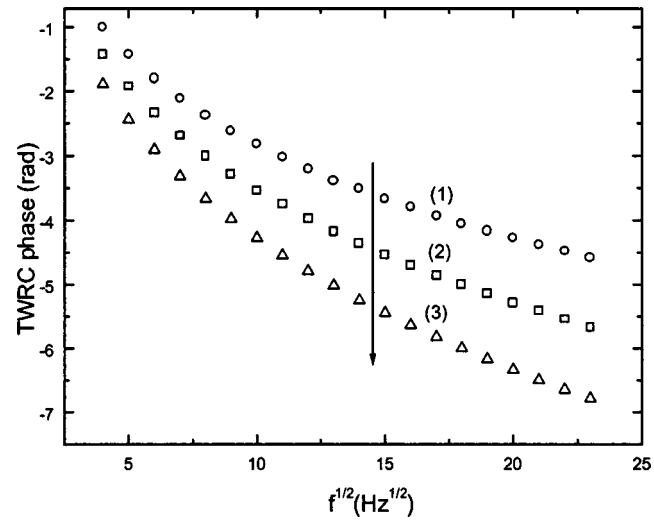

FIG. 7. TWRC signal phases for distilled water at three different intracavity sample thicknesses. Cavity length increases in the direction of the arrow. The differences between these thicknesses are 50 μm.

The same analysis was performed for the case of the photopyroelectric phases. Figure 7 shows the phase lags for the foregoing distilled water samples. Figure 8 shows the corresponding phase differences, the continuous lines corresponding to best fits to Eq. (7). The results are summarized in Table I. The average values for the thermal diffusivity of distilled water at 26 °C from the amplitude and phase (columns 4 and 5 in Table I) are $0.001\,48 \pm 0.000\,05$ cm^2/s and $0.001\,44 \pm 0.000\,04$ cm^2/s, respectively. Those for ethylene glycol are $0.000\,96 \pm 0.000\,04$ cm^2/s and $0.000\,96 \pm 0.000\,04$ cm^2/s, respectively. It is seen that the precision of the TWCR self-normalizing technique is up to the third significant figure, primarily on account of the absence of competing signal generation mechanisms and microphonic noise. A comparison with literature values is also shown in column 6 of Table I. The precision of the TWRC self-normalization method is compromised by one significant figure with respect to single cavity-scan measurements,[5] due to the noise statistics introduced by the independent measurements at two different cavity lengths. Any possible synchronous acoustic effects of hydrostatic pressure modulation within the TWRC due to thermal expansion/contraction cycles of the aluminum foil on the PVDF signal were considered. They were found to be negligible since the signal was zero at cavity lengths much larger than the thermal diffusion length in the liquid.

V. CONCLUSIONS

Two sample-thickness self-normalizing photothermal methodologies for measuring the thermal diffusivity of materials have been presented. The self-normalization procedures eliminate the instrumental transfer function efficiently. This feature represents significant simplification and measurement precision advantages for the analysis of data over conventional externally normalized frequency-scanned photothermal techniques. The methodologies were applied to the

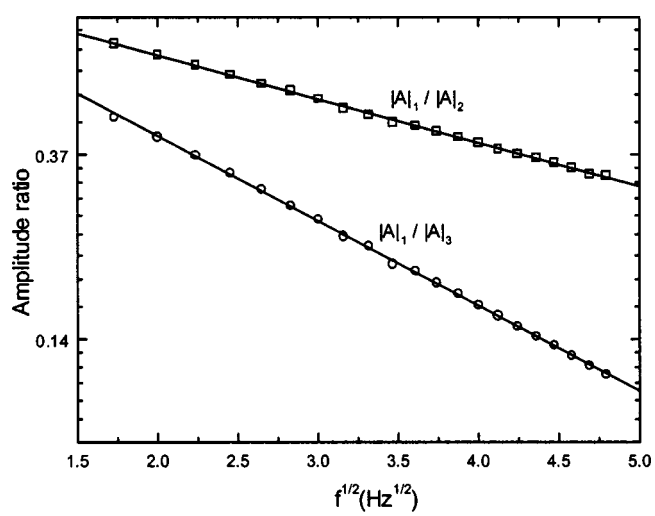

FIG. 6. TWRC signal amplitude ratios for the distilled water samples of Fig. 5. The subscript numbers correspond to the curves of Fig. 5. The continuous straight lines are the best fits to Eq. (6).

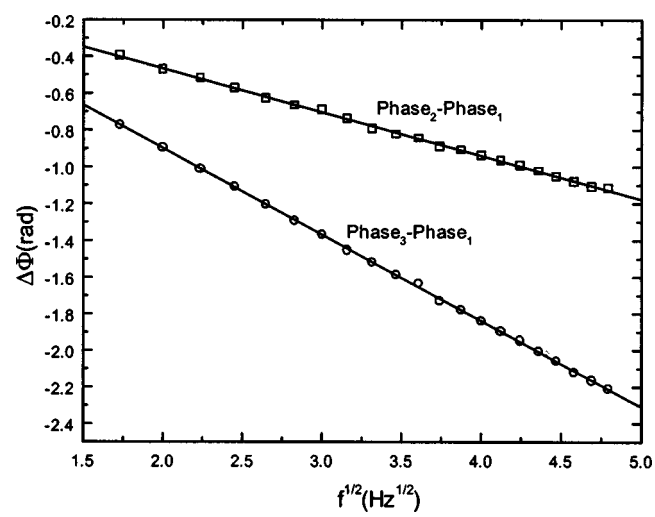

FIG. 8. TWRC signal phase differences for the distilled water samples of Figs. 5 and 7. The subscript numbers correspond to the curves of Fig. 5 and 7. The continuous straight lines are the best fits to Eq. (7).

Downloaded 18 Jul 2008 to 128.100.49.17. Redistribution subject to AIP license or copyright; see http://jap.aip.org/jap/copyright.jsp

open-cell photoacoustic configuration for measuring the thermal diffusivity of dental resins and to the photopyroelectric thermal-wave resonant cavity technique for the measurement of thermal diffusivity in liquids.

As opposed to the OPC technique, the TWRC technique does not involve a thermoelastic signal component. As a result, the measurement precision achieved is two- and three-significant figures, respectively. Precision improvements on the OPC configuration could be achieved by suppressing the thermoelastic expansion mechanism. Furthermore, the TWRC technique can also be applied to incompressible solid samples, provided adequate thermal coupling between the sample and the pyroelectric surface is obtained. Two samples of the same material of different thicknesses are needed in order to implement both techniques. Our use of dental resins to test the OPC technique reflects their growing importance for restoration work. The rapid development of dental materials makes it important to implement simple methodologies to characterize critical thermal loads in dental practice. Therefore, simple photothermal methodologies for thermophysical property measurements of these materials are of practical value. Furthermore, simple and highly sensitive thermal characterization of liquids such as water samples may be of value to the health and environmental sectors.

ACKNOWLEDGMENTS

The authors wish to acknowledge the support of the Natural Sciences and Engineering Research Council of Canada (NSERC) through a Research Grant. One of us (J. A. B-L.) further wishes to thank the Consejo Nacional de Ciencia y Tecnología (CONACyT) of Mexico for partial support of this work through a Postdoctoral Grant.

[1] A. C. Tam, Rev. Mod. Phys. **58**, 381 (1986).
[2] *Progress in Photothermal and Photoacoustic Science and Technology*, Vol. I, edited by A. Mandelis (Elsevier, New York, 1992).
[3] H. Vargas and L. C. M. Miranda, Phys. Rep. **161**, 43 (1988).
[4] J. Caerels, C. Glorieux, and J. Thoen, Rev. Sci. Instrum. **69**, 2452 (1998).
[5] G. Pan and A. Mandelis, Rev. Sci. Instrum. **69**, 2918 (1998).
[6] C. H. Wang and A. Mandelis, Rev. Sci. Instrum. **70**, 2372 (1999).
[7] J. A. Balderas-López, A. Mandelis, and J. A. García, Rev. Sci. Instrum. **71**, 2933 (2000).
[8] J. A. Balderas-López, G. Gutiérrez-Juárez, M. R. Jaime-Fonseca, and F. Sánchez-Sinencio, Rev. Sci. Instrum. **70**, 2069 (1999).
[9] J. A. Balderas-López *et al.*, Forest Prod. J. **46**, 84 (1996).
[10] S. Bibriesca, R. Equihua, and L. Villasenor, J. Eur. Ceram. Soc. **10**, 1979 (1999).
[11] M. V. Marquezini, N. Cella, A. M. Mansanares, H. Vargas, and L. C. M. Miranda, Meas. Sci. Technol. **2**, 396 (1991).
[12] L. F. Perondi and L. C. M. Miranda, J. Appl. Phys. **62**, 2955 (1987).
[13] A. Rosencwaig and A. Gersho, J. Appl. Phys. **47**, 64 (1976).
[14] J. Shen and A. Mandelis, Rev. Sci. Instrum. **66**, 4999 (1995).
[15] F. A. McDonald and G. C. Wetsel, Jr., in *Physical Acoustics, Principles and Methods XVIII*, edited by W. P. Mason and R. N. Thurston (Academic, San Diego, CA, 1988), Chap. 4, pp. 167–277.
[16] S. Civjan, J. J. Barone, P. E. Reinke, and W. J. Selting, J. Dent. Res. **51**, 1030 (1972).
[17] C. A. Pelá, S. Rocha, E. de Paula, and O. Baffa, Rev. Sci. Instrum. **69**, 3392 (1998).
[18] Y. S. Touloukian, R. W. Powell, C. Y. Ho, and M. C. Nicolau, *Thermal Diffusivity* (IFI/Plenum, New York, 1973).
[19] E. R. G. Eckert and R. M. Drake Jr., *Analysis of Heat and Mass Transfer* (Hemisphere, New York, 1978).

Downloaded 18 Jul 2008 to 128.100.49.17. Redistribution subject to AIP license or copyright; see http://jap.aip.org/jap/copyright.jsp